Submitted to *Journal of Climate*.

Local Modes of Atmospheric Variability: A Case Study of Southern California

SEBASTIEN CONIL*

Sebastien CONIL, Dpt of Atmospheric and Oceanic Sciences, UCLA

ALEX HALL

Alex HALL, Dpt of Atmospheric and Oceanic Sciences, UCLA

(27 April 2005)

ABSTRACT

We examine the primary modes of local atmospheric variability in a 6-km regional atmospheric model of the southern third of California, an area of significant land surface heterogeneity, intense topography, and climate diversity. The model was forced by reanalysis boundary conditions over the period 1995-2003. The region is approximately the same size as a typical grid box of the current generation of general circulation models used for global climate prediction and reanalysis product generation, and so can be thought of as a laboratory for the study of climate at spatial scales smaller than those resolved by global simulations and reanalysis products. We find that the simulated circulation during the October to March wet season, when variability is most significant, can be understood through an objective classification technique in terms of three wind regimes. The composite surface wind patterns associated with these regimes exhibit significant spatial structure within the model domain, consistent with the complex topography of the region. These regimes also correspond nearly perfectly with the simulation's highly-structured patterns of variability in hydrology and temperature, and therefore are the main modes of local climate variability. The regimes are approximately equally likely to occur regardless of the phase of the classical large-scale modes of atmospheric variability prevailing in the Pacific–North American sector. The high degree of spatial structure of the local regimes and their tightly-associated climate impacts, as well as their ambiguous relationship with the primary modes of large-scale variability demonstrates that the local perspective offered by the high resolution model is necessary to understand and predict the climate variations of the region.

1. Introduction

Perhaps partly because the current global reanalysis products and the current generation of general circulation models have typical resolutions on the order of a few hundred km, studies of climate variability have generally focused on modes with spatial scales larger than 1000 km. Smaller spatial scale climate variability can then be accounted for to the extent it is correlated with the large scale mode and can therefore be understood as an impact of it (e.g. Redmond and Koch, 1991; Thompson and Wallace, 2001; Hall and Visbeck, 2002). In this study we examine the hypothesis that climate variability on the regional scale (< 500 km) can instead be understood in terms of highly-structured local modes that bear little relationship to well-established large-scale modes of climate variability.

Our laboratory for examining this hypothesis is Southern California, a region rich in local atmospheric phenomena. Influenced by the strong subtropical high over the adjacent North Pacific ocean, Southern California climate from April to September is warm, dry, and stable. Winds blow steadily alongshore from the Northwest and the large-scale sinking motion almost completely suppresses precipitation. The stability of the April to September dry season contrasts markedly with the highly variable conditions during the local wet season, from October to March. During this half of the year, the North Pacific high moves south and its intensity decreases. This sets the stage for synoptic conditions during which moist onshore flows bring precipitation. In fact, this half of the year accounts for almost all of Southern California's annual mean rainfall (Cayan and Roads, 1984). However, during this season, the steady alongshore winds of the North Pacific subtropical high are interrupted not only by moist precipitation-generating onshore flows, but also by strong offshore flow events known as 'Santa Ana winds' (Sommers, 1978; Raphael, 2003). The source of the air in these events is the high desert interior of the American West rather than the North Pacific Ocean, creating extremely dry conditions along the Southern California coast. Thus from October to March, the Southern Californian often finds the famous pleasant

**Corresponding author address:* Sebastien CONIL Dpt of Atmospheric and Oceanic Sciences, UCLA 405 Hilgard ave, Los Angeles, CA 90095-1565 USA Email:conil atmos.ucla.edu

climate of the region perturbed by heavy and prolonged precipitation events favoring flooding and landslides (Cannon, 2001), as well as extreme hot, dry and windy days favoring wildfire (Westerling et al., 2004). Because of the much larger atmospheric variability during the October-March season (Winant and Dorman, 1997) and its significance for humans and ecosystems, we focus on this half of the year in our study of local modes of atmospheric variability.

These local atmospheric circulation anomalies exhibit a large degree of spatial structure, undoubtedly due to the spatial heterogeneity of Southern California surface conditions. The region has complex topography, including large mountain complexes, low-lying coastal and interior plains, and high desert plateaus (Fig. 1). There is also large variation in surface type: Ocean, highly urbanized land areas, zones of intensive agriculture, forests, and deserts are all found within Southern California. This surface heterogeneity is linked not only to structure in the circulation, but also to significant diversity of local climate, being both the cause and the consequence of large and persistent spatial gradients in temperature and hydrology.

So much spatial variability calls for datasets with high spatial resolution. However, surface observations are sparsely distributed (see Fig. 2), plagued by gaps in temporal coverage, and often not taken for long enough periods to provide stable climate statistics. Furthermore the number of climate variables recorded at these stations is often small, restricting the scientific scope of investigations based on them. As the highest resolution reanalysis product, the North American Regional Reanalysis is a possible alternative. However, its 32 km resolution is approximately the same as the largest characteristic spatial scales of Southern California's surface heterogeneity and major mountain complexes (Fig. 1). Therefore it cannot be expected to describe adequately the region's circulation or climate (Leung and Qian, 2003; Leung et al., 2003). To circumvent these barriers to the study of local climate, we imposed the large-scale conditions of the Eta 40 km-resolution reanalysis over the Western U.S. on a regional atmospheric model with 6-km grid spacing. Since this resolves the most important geographical features of the region, we hypothesized that this was also high enough to resolve the most important features of the local atmospheric circulation. We confirmed this by validating the simulation's wind anomalies against available observations. Our simulation runs for the beginning of availability of the Eta model reanalysis in 1995 through the year 2003. This provides a long enough time series to provide a statistically stable description of local modes of synoptic variability. We present further details about the design of our Southern CA regional climate simulation and its validation in section 2.

The first goal of our study is to describe the Southern California wet season atmospheric variability in an objective way. Empirical Orthogonal Function (EOF) analysis is a standard technique to describe large-scale modes of atmospheric variability such as the Northern and Southern Annular Modes and the Pacific North American pattern (e.g. Barnston and Livezey, 1987; Thompson and Wallace, 2000). However, this technique is inappropriate for Southern California because circulation variability here cannot be characterized as oscillations between the positive and negative phases of modes of variability. At first glance, it appears that it would be appropriate to think of the offshore Santa Ana mode and the onshore precipitation mode as the positive and negative phases of a single mode of variability. However, it turns out that in our simulation the offshore winds of the Santa Anas are not symmetric to the onshore winds of precipitation events, either in their mean pattern or their variability. Moreover, even if these patterns were symmetric, they are present only intermittently, the flow normally being characterized by a steady alongshore breeze. This asymmetry and intermittency cannot be captured through standard EOF analysis, which is based on linear asumptions. We therefore adopt cluster analysis to identify the dominant modes of circulation variability (Gong and Richman, 1995; Smyth et al., 1999). This technique allows us to capture the dominant modes in terms of regimes that are not necessarily symmetric to one another in either the space or time domains. We describe the cluster analysis technique and the three local wind regimes it identifies in section 3.

The second goal of our study is to relate local wind modes to local climate variability. In section 4, we demonstrate that the three local wind regimes identified by the cluster analysis are the main sources of local climate variability, having a nearly one-to-one relationship with anomalous patterns of humidity, precipitation, and temperature. The climate impacts of the local wind regimes exhibit a large degree of spatial structure that can only be revealed with high resolution information, a further rationale for using our 6-km resolution model to study Southern California's climate.

The final goal of our study is to characterize the relationship of the local wind regimes to classical larger-scale modes of climate variability. We do this in section 5, and conclude that the local modes largely do not coincide in any systematic way with anomalies in the larger-scale modes. Instead the local wind regimes are particularly sensitive to a peculiar monopole pressure pattern centered in the Western U.S. which apparently

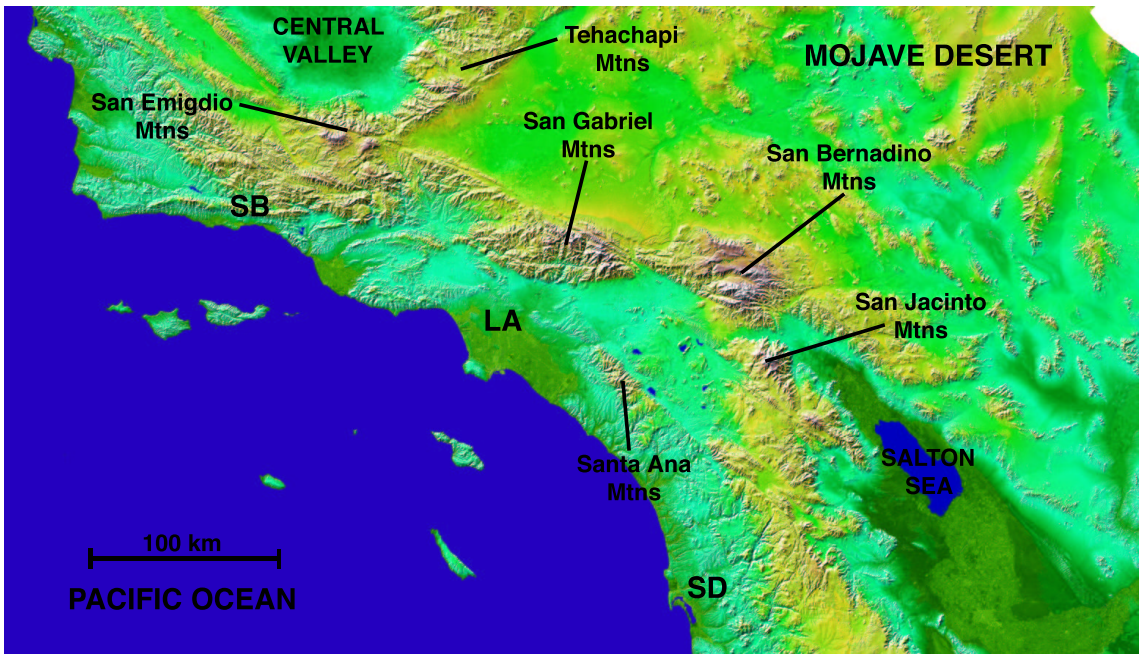

FIGURE 1: The geography of Southern California. The region shown matches the innermost 6-km resolution domain of the simulation. Elevation is indicated as color, with dark green corresponding to sea level or below, and reddish brown corresponding to the highest elevations (approximately 2.5-3 km). Among other major features, the main mountain complexes are labeled, as well as three cities: Santa Barbara (SB), Los Angeles (LA), and San Diego (SD). The Channel Islands can be seen in the Southern California Bight. This image was generated by the NASA/JPL Shuttle Radar Topography Mission.

can be excited by any of the classical large-scale modes.

In section 6 we present concluding remarks.

2. Regional Climate Simulation

a. *Experimental design*

A high-resolution simulation of Southern California climate was performed with version 3 of the PSU/NCAR mesoscale model (MM5). Three nested grids of increasing resolution were implemented over the Western United States and Southern California, each with 23 vertical levels. The larger domain covers most of the Western United States at 54-km resolution. It extends from Southern Baja California (27.5°N) in the south to Oregon (43.5°N) in the north. Its eastern boundary is located over western Colorado (110°W) while the western boundary (128°W) is located far enough over the Pacific ocean to include equivalent ocean and land areas. The intermediate domain has an 18-km resolution and covers most of the California region and ajacent ocean, from 31°N to 37°N and from 113°W to 123°W. The 6-km-resolution inner domain zooms in on Southern California. It has 94 grid cells in the zonal direction and 56 grid cells in the meridional direction. Fig. 2 shows the topography in the inner domain. A comparison with Fig. 1 reveals that the main mountain complexes of Southern California, including the San Bernadino, San Gabriel, Tehachapi, San Jacinto, and Santa Ana mountains are resolved at 6 km.

MM5 includes a large number of physics parameterization options. In all three domains we used the Dudhia simple ice microphysics scheme for moisture prediction and the counter gradient turbulence scheme. In the two outer domains we used the Kain-Fritsch cumulus parametrization, while in the inner domain no cumulus parameterization was used. The initial atmospheric states the lateral boundary conditions, and the sea surface temperatures (SSTs), all with a nominal horizontal grid resolution of 40 km, were derived from the Eta analysis obtained through NCAR's GCIP Model Output Archive. Updated lateral conditions are available every 3 hours from this archive, and we interpolated them in time prior to imposing them on the model. SSTs were updated every 3 days. The model output was archived at hourly intervals. The time period of the simulation extends from May 1, 1995 to December 31, 2003. The simulation can therefore be thought of as a high-resolution reconstruction of Southern California atmospheric conditions over this time period, consistent with our best estimate of the large-scale conditions, the topography resolved at 6-km

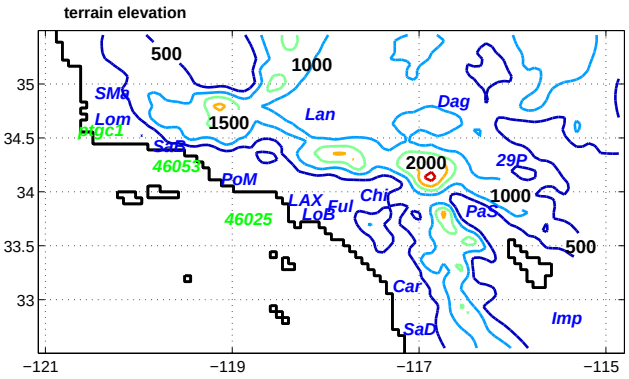

FIGURE 2: The topography of the innermost 6-km resolution domain. The model coastline is shown to give an idea how well model discretization resolves the land-ocean boundary. Los Angeles is located approximately at the center of the domain, and San Diego at the south near 117°W. The Channel Islands of the Southern California Bight can also be seen. The water feature in the southeast part of the domain is the Salton Sea. The locations of the wind observations used for the model validation in section b are also shown. Contour intervals = 500m.

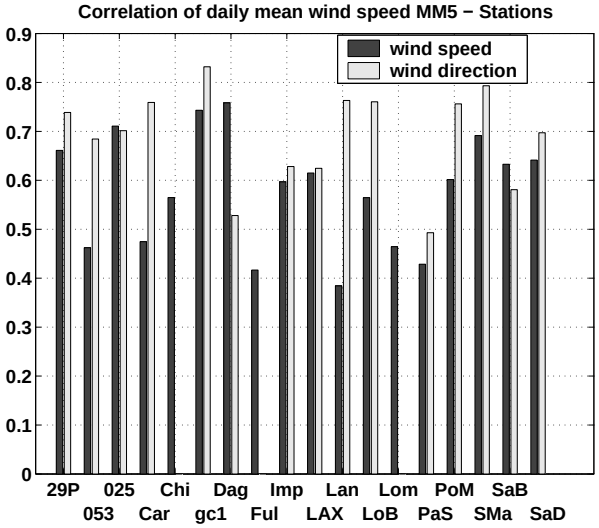

FIGURE 3: The correlations between daily-mean near-surface wind speed and direction anomalies observed at the stations shown in figure 2 and the daily-mean wind speed and direction anomalies simulated at the closest grid points during the 8 October-March wet seasons from 1995-2003. Stations Chi, Ful, and Lom, have fewer than 100 data points on wind direction, so wind direction correlations were not computed at these locations.

resolution, and the physics of the MM5 model.

b. *Validation*

From the hourly model outputs we computed the daily-mean, near-surface wind anomalies from a composite seasonal cycle, focusing on the wet season, from October to March. We used daily averages of the wind to remove the influence of the local diurnal circulation, including the land/sea breeze and diurnal mountain winds. We compared these simulated daily-mean wind anomalies with the daily-mean wind anomalies observed at 16 stations over land and 2 buoys over the ocean. The station and buoy data were provided by the National Climate Data Center and the National Data Buoy Center. The simulated and observed winds are highly coherent throughout the 6-km domain. For example, we computed the correlations between wind direction anomalies observed at the stations and the wind direction anomalies simulated at the closest grid points during the 8 October-March wet seasons from 1996-2003 (figure 3, light grey bars). In all cases but one the correlations are greater than 0.5, and are generally much higher, averaging around 0.7. In the case of wind speed (figure 3, dark grey bars), the correlations are above 0.4 at all 18 locations, while for 10 locations they are above 0.6, the highest correlation reaching almost 0.8.

Aside from errors in the simulation arising from model formulation, the correlations may not be absolutely perfect for two reasons closely related to the verification methodology (e.g. see Mass et al., 2002). First, the station wind data are subject to systematic and random measurement error. Unfortunately this error is nearly impossible to quantify because the ultimate data sources are so disparate. Second, there may be small-spatial-scale wind variability resulting from complex topography unresolved at 6 km. In this case, wind field discrepancies between the observed point and the conditions averaged over a 6 km square grid box including that point, represented by model output, could become important. We have preliminary evidence of this effect. When the station wind data are correlated with a 2-km simulation of Southern California similar in design to the simulation analyzed in this paper for the year 2002 only, the correlations in wind speed and direction (not shown) do generally increase. However, the increase is modest (only about 0.05), suggesting that this effect is not the main reason the correlations are not perfect. We therefore conclude that it would be unlikely that the skill of the model would improve a great deal if we performed the entire simulation at 2 km resolution or higher. This may be because the typical spatial scale of Southern California mountain complexes is on the order of tens of kilometers (see Fig. 1), so that 6 km grid spacing resolves the main features of the topographic perturbations to the atmospheric flow. However, in other regions

where the topography has relatively more variance on smaller spatial scales than Southern California, resolutions higher than 6 km may offer greater realism.

In spite of these additional sources of disagreement beyond simple model formulation error, observed and simulated wind direction and speed at locations scattered widely throughout the domain agree quite well. This gives confidence that the local wind regimes we identify in section 3 based on model output are representative of the actual wind regimes in Southern California: The magnitude and direction of the wind anomalies associated with them are reasonably accurate, as is their timing and their probability of occurrence. Since the stations shown in Fig. 2 are more or less randomly distributed through the model domain, it is also highly likely that if there were stations corresponding to every model grid point, and we computed correlations between model and observation wind speed and direction, they would be as high as those shown in figure 3. Therefore the simulation provides the most accurate and densely sampled information about Southern California weather and climate from the period 1995-2003 available at the present time.

3. Local Wind Regimes

a. *Preliminary EOF analysis*

As noted in section 1, the atmospheric circulation over Southern California is highly variable in the wet season. Fig. 4 shows the standard deviation of the daily-mean, near-surface wind speed anomalies in the 6-km resolution domain over the 8 October-March periods from 1995 to 2003. The anomalies were calculated as departures from a composite seasonal cycle. Over land, the wind variability distribution corresponds closely to the topography. The std dev of wind speed exceeds 2.1 m/s over the main mountain complexes of Southern California, while over low-lying terrain, including the Central Valley, the Coachella valley, and the urbanized coastal zone, wind variability is suppressed, with the std dev being on average about half as large as at high elevations. Mass conservation forces the flow to occupy a smaller vertical extent as it makes its way over mountain complexes. This would strengthen the overall flow, including that of the surface, over high elevations. This effect would enhance wind speed variability at high elevations as large-scale conditions force flow over mountain complexes from different directions, perhaps accounting in part for the pattern in Fig. 4. The wind variability may also be larger at high elevations because the planetary boundary layer is thinner and subject to greater exchange with the free atmosphere there, so that surface wind speeds bear a greater imprint of the larger flow variability of the free atmosphere than at low elevations. The ocean generally exhibits much more wind speed variability than the land, with the highest wind speed variability of the entire domain visible south and west of Santa Barbara. //

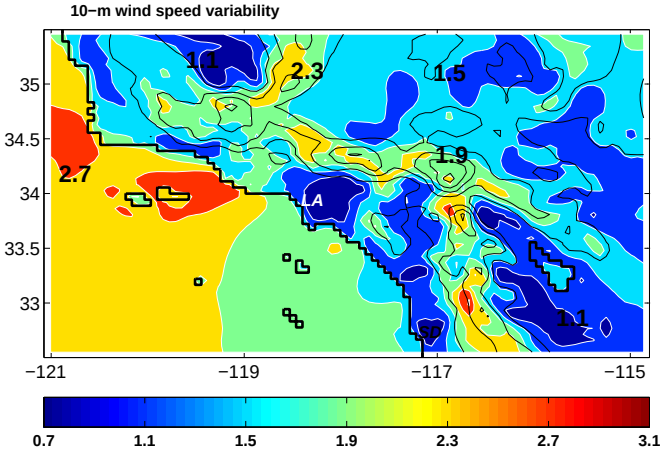

FIGURE 4: St dev of the daily mean 10m wind speed for the wet season (October-March) over the period 1995-2003 simulated in the 6-km Southern California domain. Units: m/s. The topography is shown in black contours (intervals = 500 m).

As noted in section 1, we use a cluster analysis technique to identify the main wind regimes generating the variability seen in Fig. 4. The first step of cluster analysis is to do a real vector EOF analysis (Kaihatu et al., 1998; Ludwig et al., 2004) to minimize the number of degrees of freedom of the data. The EOFs were computed from the covariance matrix of the daily-mean, near-surface wind anomalies for the wet-season period over the 6-km resolution domain.

The two EOFs accounting for the most variance are shown in figure 5. The first EOF accounts for nearly 39% of the variance and is significantly well separated (according to the North et al., 1982, Rule of Thumb) from the second EOF, which accounts for 32% of the variance. The second EOF, in turn, is also significantly separated from the third EOF which accounts for only 8% of the variance. The wind pattern of the first EOF is characterized by strong northeasterly offshore flow from the Great Basin into the coastal zone and out over the ocean. Since the mean winds have a weak cross-shore component, this pattern is similar to the cross-shore component of the actual winds that occur when the principal component associated with the first EOF (PC1) is positive. The flow patterns associated with positive PC1 therefore correspond roughly with classic Santa Ana conditions.

Conversely, when PC1 is negative it corresponds to onshore flow, likely moisture-laden since it originates over the ocean. The wind pattern of the second EOF is characterized by northwesterly flow over the ocean and weak anomalies over land, except at high elevations where the flow is predominantly northerly. The alongshore component of the mean flow over the ocean is northwesterly (Caldwell et al., 1986, Dorman and Winant, 1995) and is strong enough that the second EOF captures variations in the direction and intensity in these winds but rarely represents a reversal of the flow to southeasterly conditions, even when values of the principal component associated with the second EOF (PC2) are negative.

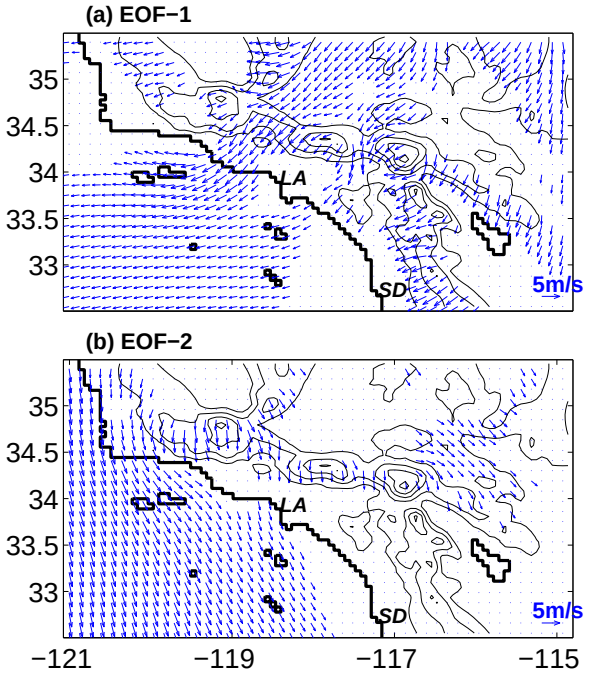

FIGURE 5: The first two EOFs of the daily mean 10 m wind speed anomalies for the wet season (Oct-Mar) over the period 1995-2003 simulated in the 6-km Southern California domain, shown as regression maps. Units: m/s. The first (second) EOF accounts for 39% (32%) of the wind variability. The topography is shown in black contours (intervals = 500 m). Every other grid point in both zonal and meridional directions is suppressed here for clarity.

b. *Cluster analysis*

We perform the cluster analysis using two distinct and independent classification techniques. One method is the k-means algorithm of Michelangeli et al. (1995) and the other is the probabilistic clustering scheme of Smyth et al. (1999), based on finite mixture models. These two schemes were applied to a varying number of leading wind EOFs (from 2 to 8) and for a varying number of clusters (from 2 to 8). The two methodologies are able to provide a criterion giving the optimal number of clusters describing the data. The two classification methods both give an optimal number of clusters somewhere between 3 and 5. The best agreement between the two methods was found using the 2 first EOFs (those shown in Fig. 5, and together accounting for almost 75% of the variance) classified in 3 clusters. We verified that these results are insensitive to clustering parameters or the domain of the analysis. We will present the results of the mixture model clustering because it has several advantages compared to the k-means scheme (Kondrashov et al., 2004)., which was merely used as an independent verification of the results.

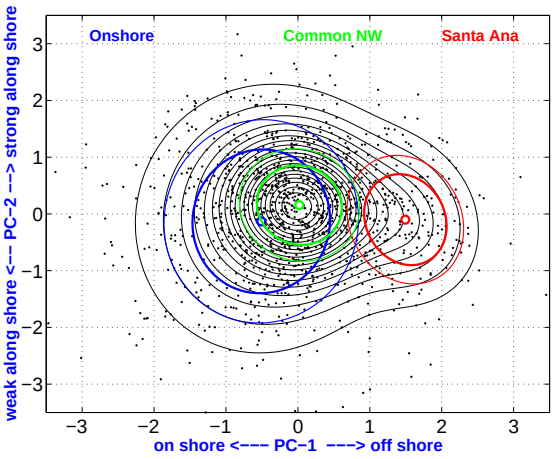

FIGURE 6: Scatterplot of the daily wind, near-surface anomalies in PC1–PC2 space for the 8 winters (black dots). The PDF estimate of the data distribution in PC1–PC2 space provided by the mixture model is shown with black lines. Estimated centroids of the three clusters is indicated by the small colored circles. The extension of the clusters is indicated by the covariance ellipsoids, corresponding to semi axes equal to 1 (heavy colored lines) and 2 (light colored lines) times the st dev in each principal direction.

Each day of the 8 wet seasons is associated with values of PC1 and PC2. We present these values in scatterplot format in PC1-PC2 subspace in Fig. 6. This figure also shows the probability distribution function (PDF) of the data in PC1-PC2 space estimated by the mixture model using the first 2 EOFs and 3 clusters. The ellipsoids of Fig. 6 define membership in one of the three clusters defined by the mixture model. The mean of the clusters in PC1-PC2 space is described by the position of the ellipsoid centers, while their variance is described by the size of the ellipsoids. The distribution of the points

and the associated PDF structure show that while most of the days are concentrated near the origin where the PDF reaches its maximum, perturbations to this state occur toward positive PC1. Simultaneous anomalies in PC2 are relatively uncommon, resulting in a narrow and protruding lobe of the PDF toward positive PC1. Perturbations toward negative PC1 also occur, but are associated with large excursions of PC2 in either the positive or negative PC2 directions. This creates an asymmetry in the overall PDF with respect to the line of zero values of PC1, a feature of the PDF reflected in the cluster definitions.

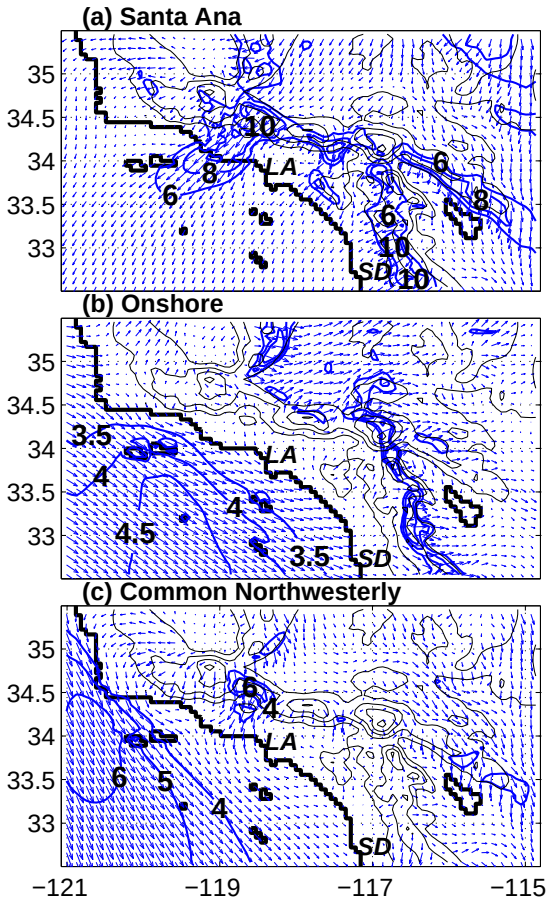

FIGURE 7: 10m wind composite maps for the three wind regimes generated by the mixture model shown in Fig.6. The blue contours show the wind speed (units: ms^{-1}). The topography is shown in black contours (intervals = 500 m). Every other grid point in both zonal and meridional directions is suppressed here for clarity.

The mixture model allows us to determine membership of any data point in one of the three clusters by measuring how close the point is to the center of the ellipsoids of Fig. 6. Adopting a threshold distance from the centers of the ellipsoids (in this case two standard deviations from the center), we then have an objective means of determining whether the winds on any particular day can be classified as belonging to one of the three clusters. The first regime, which we call the Santa Ana regime (red ellipsoids), occupies a region of positive values of PC1 and therefore is associated with offshore flow. The second regime is shifted toward negative values of PC1 and slightly negative values of PC2. Its extension, shown by the blue ellipsoids, is larger than the other two regimes, meaning that it represents a larger variety of conditions, though they have in common a predominant onshore flow. We call this the Onshore regime. The extension of the third regime, shown by the green ellipsoids, is relatively small, so that the wind patterns of this regime are not as diverse as the other two clusters. As we show below, the majority of the data points belong to this cluster. Moreover, the third regime is associated with very small anomalies in PC1 and PC2. This implies that the wind fields associated with this cluster have a weak cross-shore component and a significant northwesterly alongshore component. Because this regime is so common and is so similar to the northwesterly winds of the climatology, we call it the Common Northwesterly regime. Our definition of the clusters implies that less than 3% of the days are not classified.

After classifying the days, we then averaged the wind fields of the days belonging to each cluster to create composite wind patterns. The composite wind pattern of the first regime (Fig. 7a) is typical of Santa Ana conditions with strong northeasterly flow (Hu and Liu, 2003) , reaching 10 m s^{-1} over the highest elevations of the coastal range throughout the entire domain. The strongest area of offshore flow is seen just to the northwest of Los Angeles, where air is channeled through an area of rough but relatively low-lying topography between the higher San Gabriel and San Emigdio mountain complexes. Over the ocean, these winds are also blowing from the northeast but are weaker. In the larger 18-km resolution parent domain, northeasterly winds are associated with the days of the Santa Ana cluster on the western slopes of the southern Sierra Nevada, in northwestern Baja California (Travisña et al., 2003) and over the Gulf of California (not shown). Northeasterly flow is not found beyond these regions on Santa Ana days in either the 18-km or 54-km resolution parent domains.

In the Onshore regime (Fig. 7b), the winds over the ocean develop a westerly component, so that an onshore component prevails along the coast. In the coastal zone between the shore and the coastal ranges, the wind anomalies are very small. Then on the eastern side of the

coastal ranges the strong onshore component reappears. This pattern is consistent with the development of barrier jets parallel to the coastal mountain ranges in the coastal zone. The onshore flow is forced to surmount the barrier flow in addition to the topography, so that at the surface the onshore signature disappears in the area of the blocked flow. Once the onshore flow passes the peak of the coastal range, the barrier flow is no longer present, and so the onshore flow reappears in the surface wind field. This interpretation is confirmed by the presence of strong onshore flow at higher altitudes during the days classified as belonging Onshore regime (not shown). Later we also show that this interpretation is consistent with the precipitation patterns associated with the Onshore regime. The last regime (Fig. 7c) is dominated by strong northwesterly winds over the ocean. Evidence of offshore flow is seen over the coastal range; however the anomalies are very small compared to those of the Santa Ana regime. Elsewhere on land the surface wind anomalies of the Common Northwesterly regime are generally small.

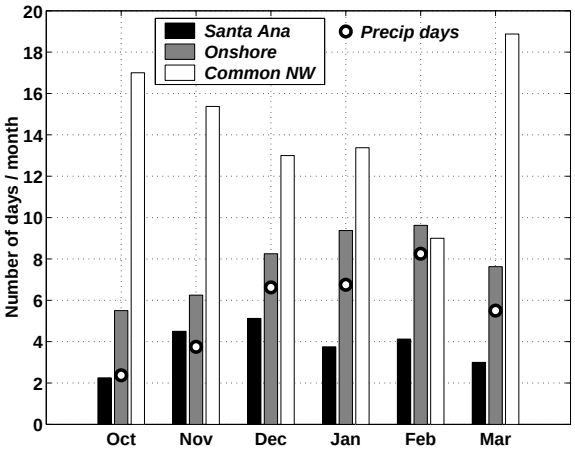

FIGURE 8: The monthly mean occurrence of the local wind regimes and the monthly mean numbers of precipitation days during the wet season, simulated in the inner domain.

The seasonal cycle of the occurrence of the three wind regimes, expressed as the average number of days per month belonging to each cluster, is presented in Fig. 8. We emphasize that since we removed the seasonal cycle from the wind data prior to performing the cluster analysis, this represents the seasonal cycle of wind variability, rather than the seasonal cycle of the mean winds. Approximately 2 to 5 days per month belong to the Santa Ana regime, corresponding to 14% of the days. The number of Santa Ana days increases throughout early winter, and is largest in December before tapering off through March. Raphael (2003), defining a Santa Ana event as one where the observed pressure gradient between the Great Basin and the Southern California coast exceeds a certain threshold, found a very similar seasonal cycle in the Santa Anas. This is additional confirmation that the simulation is reproducing the statistics of observed variability with high degree of fidelity, and that our Santa Ana cluster corresponds to a previously-known physical mode of variability. The Onshore regime is about twice as common as the Santa Ana regime, comprising 29% of the wet-season days on average. It increases in frequency from October, when approximately 5 days belong to the Onshore regime, to February, when nearly 10 days do. After February the Onshore regime wanes. The seasonal cycle of the Onshore regime matches closely the seasonal cycle of the number of days when precipitation occurs. We discuss the tight relationship between the wind regimes and hydrology further in section 4. On average, most of the days (55%) belong to the Common Northwesterly regime. This regime decreases in frequency from the beginning of the wet season until February, so that during the meteorological winter months of December, January, and February, there is greater likelihood of having a day belonging to either the Onshore or Santa Ana clusters. The Common Northwesterly regime completely recovers its dominance by March.

The seasonal cycle of wind regimes shown in Fig. 8 suggests a relationship between the mean state of the circulation and its variability. At the beginning of the wet season, the Pacific subtropical high is still quite strong and variability associated with the mid-latitude jet stream is weak. The result is the predominance of the Common Northwesterly regime: steady alongshore northwesterly flow with little variability in either the alongshore or cross-shore components of the winds. As the high weakens and the mid-latitude jet stream and its vacillations strengthen over the course of late fall and early winter, this steady flow is increasingly perturbed by the Onshore and Santa Ana regimes, characterized by greater variability in both the alongshore and cross-shore components of the flow (see Fig. 6 and also the observations of wind stress variability over the Southern California Bight in Fig. 2 of Winant and Dorman, 1997). By March, variability in the alongshore and cross-shore components subsides, and the steady alongshore flow associated with the Pacific subtropical high returns.

4. Relation to Local Climate

a. *Hydrology*

Fig. 9a illustrates the connections between hydrologic conditions and the three wind regimes. The points of this figure are color-coded by the amount of rain falling that day averaged over the innermost 6 km domain. There is a tight association between hydrology and the wind regimes as defined by the isolines of probability of belonging to one of the three regimes. For example, most of the days when there is little or no precipitation have a much higher probability of belonging to the Santa Ana regime than either of the other two. Though a fraction of extremely dry days also have a significant probability of belonging to the Common Northwesterly regime, most of the extremely dry days have a negligible likelihood of belonging to the Onshore regime. Similarly, most days with substantial precipitation have the highest likelihood of belonging to the Onshore regime and negligible likelihood of belonging to the Santa Ana regime. Though some days with substantial precipitation have a significant probability of belonging to the Common Northwesterly regime, in general the meteorological conditions of the days with the highest likelihood of belonging to the Common Northwesterly regime are in between extremely dry and humid conditions. Rainfall is generally very small, though not completely negligible. On these days, a small amount of precipitation occurs somewhere in the domain, typically over the ocean in the form of drizzle from low altitude stratus clouds.

The close association between hydrology and wind regimes can be interpreted physically by examining the wind patterns and the topography of Fig. 7. During the Santa Ana regime, the source of air throughout the domain is the dry continental interior. As the dry air is forced over the coastal range and descends from the high desert to the coast, it warms adiabatically and relative humidity falls even further, virtually eliminating the possibility of precipitation. On the other hand, during the Onshore regime, the source of air is the moist Pacific. As this moist air is forced to ascend over the coastal mountain range, substantial orographic precipitation occurs. During the Common Northwesterly regime, the component of the flow across the coastal range is weak, so that neither extreme dry conditions resulting from adiabatic compression of dry desert air nor wet conditions resulting from orographically-forced condensation within moist air masses are typically associated with this regime.

Further evidence of the close association between hydrology and wind regimes can be seen in Fig. 10, which shows the number of days falling into six categories of precipitation intensity. The colored divisions indicate the number of days within each category belonging to the three wind regimes. For the lowest category of precipitation intensity, corresponding to virtually no precipitation, the vast majority of the days belongs either to the Santa Ana regime or to the Common Northwesterly regime. Going to categories of higher precipitation intensity, the fraction of days belonging to the Santa Ana regime quickly becomes negligible, and the fraction of days belonging to the Common Northwesterly regime decreases. Meanwhile the number of days belonging to the Onshore regime increases. Finally, the category corresponding to the highest precipitation intensity is overwhelmingly dominated by the Onshore regime, with 80% of the days belonging to this regime. This category in turn represents 90% of the total precipitation falling during the entire simulation, so that the overwhelming majority of total precipitation is associated with the Onshore regime.

To provide information about the geographical distribution of hydrologic conditions associated with the dry Santa Ana regime, Fig. 11b shows the composite near-surface relative humidity (RH) anomaly of the Santa Ana days. The RH anomaly is greatest in the urbanized coastal zone extending from San Diego to Los Angeles and adjacent area of the Southern California Bight, reaching values greater than 20 percentage points below the mean. There is a secondary maximum RH anomaly in the coastal zone adjacent to Point Conception, where RH typically falls about 15 to 20 percentage points below the mean. The anomaly is so large in these areas for two reasons: (1) As the desert air descends to the coast it is warmed adiabiatically, lowering its RH. (2) When the Santa Ana regime is not occurring, moist marine air often intrudes into this area, so that arrival of dry air from the desert interior implies a very large departure from the mean RH (see fig 11a).

The RH anomaly is smallest in the far eastern part of the domain, on the order of just a few percentage points. In these desert regions the air is typically dry already (Fig. 11a), and the passage of Santa Ana winds has little impact on moisture content. Moist marine air occasionally intrudes into the arid regions just north and east of the coastal range, so that a strong flow from the desert interior implies a modest reduction of RH here. The RH anomaly also decreases significantly away from the coast toward the open ocean. In the extreme southwest corner of the domain, the RH anomaly is only 5 percentage points below the mean. This is the signature of oceanic moisture being rapidly entrained

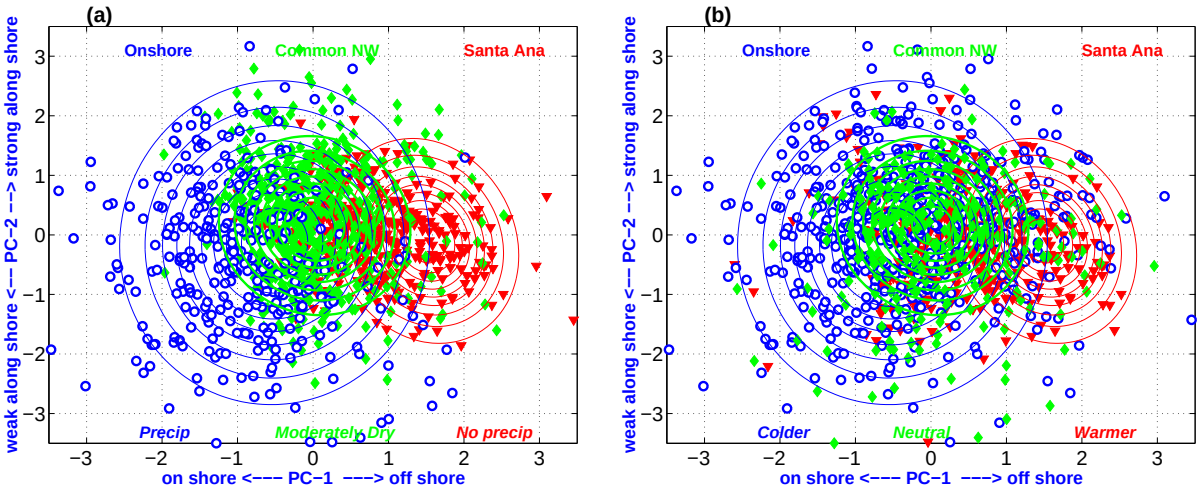

FIGURE 9: Scatterplots of the daily wind anomalies for the 8 wet seasons in PC1-PC2 space identical to fig 6, except that the points are now color-coded by (a) the daily-mean rainfall rates averaged over the 6-km domain. Red points are non precipitating or very dry days (rain rate less than 0.00005 mm/hr), green points are moderately dry or slightly precipitating days (rain rates greater than 0.00005 mm/hr and less than 0.025 mm/hr), while blue points are precipitating days (rain rates greater than 0.025 mm/hr). (b) the daily-mean 2m temperature anomalies averaged over the coastal zone between Los Angeles and San Diego. Red points are warm days (2m temperature anomalies above 0.8 ^{o}C), blue points are cool days (2m temperature anomalies below -0.8^{o}C), while the green points are neither warm nor cool (2m temperature anomalies between -0.8^{o}C and 0.8 ^{o}C). The contours of both panels (every 0.1, beginning with 0.1 and ending with 0.9) show the probability given by the cluster analysis of belonging to the Santa Ana regime (red contours), the Onshore regime (blue contours) and to the Common Northwesterly regime (green contours).

into the dry offshore flow. Fig 11b therefore gives a portrait of the spatial extent of the impact of the Santa Ana regime on hydrology. RH anomalies are small in northeast and southwest corners of the domain, while a zone of extreme dryness is confined largely to the low-lying urbanized coastal areas.

To provide information about the geographical distribution of hydrologic conditions associated with the wet Onshore regime, we show in Fig. 12 the composite precipitation on days belonging to the Onshore regime. A precipitation composite provides more information about hydrology than an RH composite in the Onshore case because, unlike the Santa Ana regime, the air is close to saturation everywhere in the domain when the Onshore regime occurs. Precipitation rates are largest on the coastal side of the coastal mountain ranges, being nearly an order of magnitude larger than the rates over the open ocean or the desert interior. This is consistent with moist onshore flow of Fig. 7b being forced over the coastal range, wringing out moisture as it ascends the mountains. A secondary maximum of rainfall is seen in the low-lying urbanized coastal zone to the south and west of the coastal range. Masi and Hall (2005), analyzing the same simulation, demonstrated that the elevated values of precipitation in the coastal zone results from the development of blocked flow parallel to the coastal ranges as low-level air masses are forced toward the interior. Once this blocked flow is in place, the moisture-laden onshore flow must surmount it in addition to the topography, enhancing precipitation well in advance of the coastal ranges themselves. They estimate that rainfall rates are typically doubled or tripled because of this effect. Analyzing individual rain events from an observational perspective, Neiman et al. (2002) and Neiman et al. (2004) also demonstrated the importance of blocking in the dynamics of the precipitation distribution in Southern California. The presence of this blocking can also be detected in the Onshore regime wind distribution of Fig. 7b: The 10-m wind anomalies are very weak on the windward side of the coastal range where blocking occurs, while strong onshore flow reappears on the lee side of the mountains.

Together, Figs. 11 and 12 reveal that the coastal zone is most affected of anywhere in Southern California by both extremes in hydrology. Parched during the Santa Ana regime, and receiving copious rainfall during the Onshore regime, this region is prone to extreme hydrologic events. Both extremes can lead to local catastrophes affecting human infrastructure, including uncontrollable wildfire, which is always associated with Santa Ana regime in Southern California (Keeley and Fother-

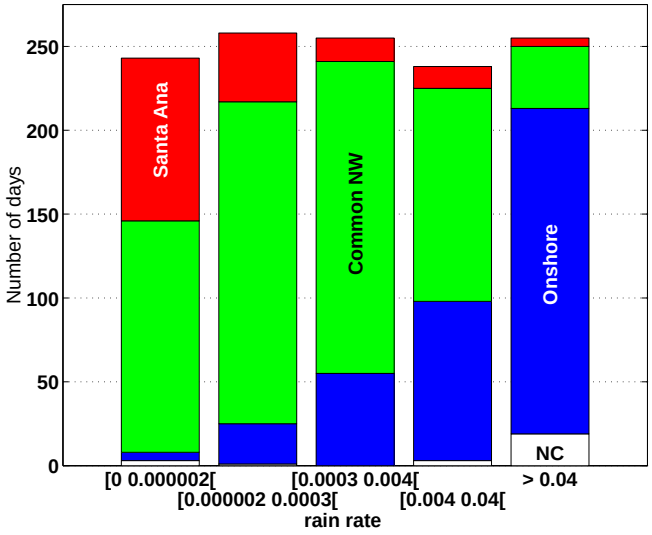

FIGURE 10: Distribution of the days according to their daily-mean precipitation rate averaged over the 6-km domain. The total height of the bars indicates the number of days experiencing a certain range of rainfall rates (mm/hr). Each bar is in turn divided into three colored parts showing the number of days within each range belonging to the Santa Ana regime (red), the Common Northwesterly regime (green) and the Onshore regime (blue). The days not belonging to any regime are left white.

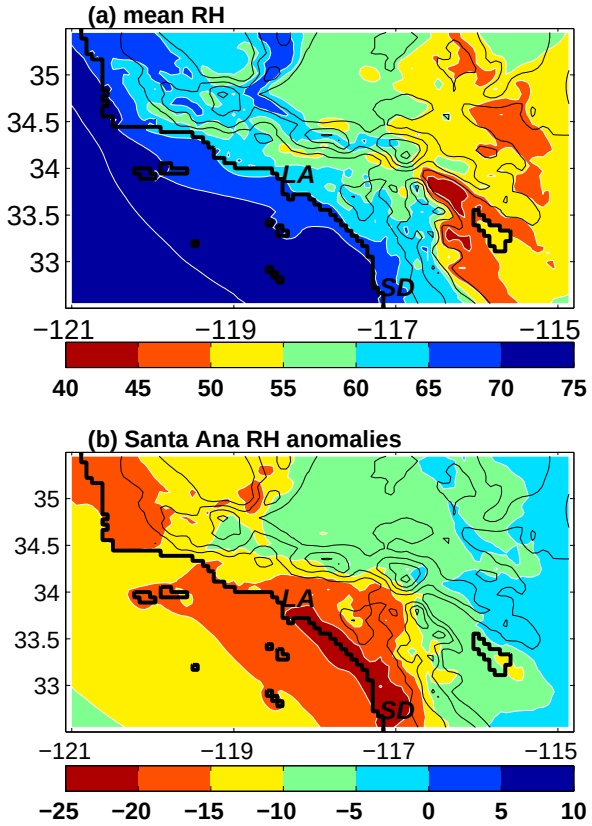

FIGURE 11: (a) Mean 2-m relative humidity during the wet season. (b) Composite 2-m relative humidity anomaly associated with the Santa Ana regime. Units: %

ingham, 2003, Westerling et al., 2004) and mudslides, which occur when rainfall saturates and destabilizes unvegetated soils on steep slopes (Cannon, 2001).

b. *Temperature*

Fig. 13 shows the near surface air temperature (SAT) anomalies associated with the three regimes. We first discuss the Onshore and Common Northwesterly regimes, and then the more complex Santa Ana case. Cold SATs are associated with the Onshore regime thoughout the 6 km domain (Fig. 13b). In contrast, warm anomalies are associated with the Common Northwesterly regime everywhere (fig 13c). The difference in the SAT signatures of these two regimes is likely attributable to differences in cloudiness between them. The largest cold anomalies of the Onshore regime, reaching values of about 3°C, are found in precisely the same regions where precipitation rates are also greatest (fig 12). These are also areas where total cloud amounts (not shown) are greatest, as expected. The resulting reduction in solar radiation leads to cooler temperatures. On the other hand, with the exception of low-level stratus clouds over the ocean, which often intrude into the low-lying coastal zone, skies are generally clear during the Common Northwesterly regime, leading to small but positive SAT anomalies.

During a typical Santa Ana event (Fig. 13a), cold SAT anomalies over the Mojave desert are likely generated by synoptic conditions of larger scale associated with the development of a high pressure center over the Great Basin (see section 5). The flow from the desert therefore brings cold air to the coastal region. However, as the air descends from the desert plateau and is channeled through the passes of the coastal ranges, it is heated by the adiabatic compression. By the time it reaches low elevations, it has been heated enough to produce anomalously warm conditions on the order of 1°C above the mean throughout the coastal zone. These anomalies are somewhat warmer than those associated with the Common Northwesterly regime (Fig. 13c).

The composite SAT patterns of Fig. 13 are representative of the actual variability in SAT in Southern California. As an illustration of this point, we show in Fig. 9b a plot identical to Fig. 9a, except now the points are color-coded by SAT in the low-lying coastal zone. Accord-

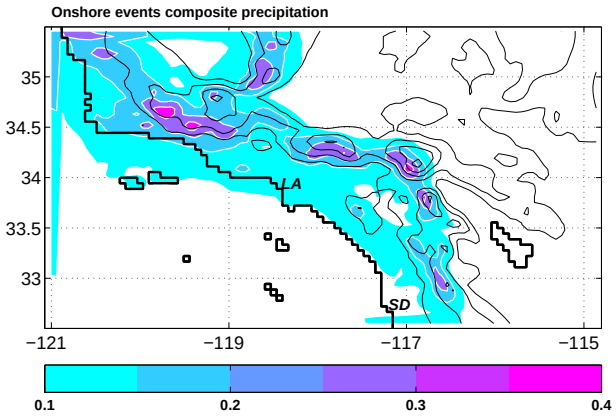

FIGURE 12: Composite precipitation distribution associated with the the Onshore regime. Units: mm/hr

ing to Fig. 13 we expect cold anomalies to be associated with the Onshore regime in this zone, warm anomalies with the Santa Ana regime, and neutral to moderately warm anomalies with the Common Northwesterly regime. Fig. 9b demonstrates that the actual temperature anomalies in this zone are indeed closely associated with the three regimes in this fashion. However, comparing panels a and b of Fig. 9, there is somewhat more variability in the SAT anomalies coinciding with any one of the regimes than in the precipitation anomalies. This is particularly apparent in the case of the Santa Ana regime. Though the majority of the days most likely to belong to this regime are significantly warmer than normal in the coastal zone, a significant fraction are also significantly colder than normal: Sometimes the desert air on Santa Ana days is cold enough that the adiabatic heating associated with its descent of the coastal range is not sufficient to produce a warm SAT anomaly at the coast. Almost all of the cold Santa Ana days are extremely dry, so that RH in the coastal zone is a better indicator of Santa Ana conditions than SAT.

Similar plots color-coded by SAT averaged over other zones of the 6-km domain (not shown) give similar results to fig 9b. Thus the three wind regimes are tightly associated not only with actual precipitation anomalies but also actual anomalies in temperature throughout Southern California. This demonstrates that the wind regimes are representative of true modes of local climate variability.

5. Relation to large-scale circulation

In this section we investigate the relationships between these local modes of climate variability and the large scale atmospheric circulation, as given by the NCEP re-

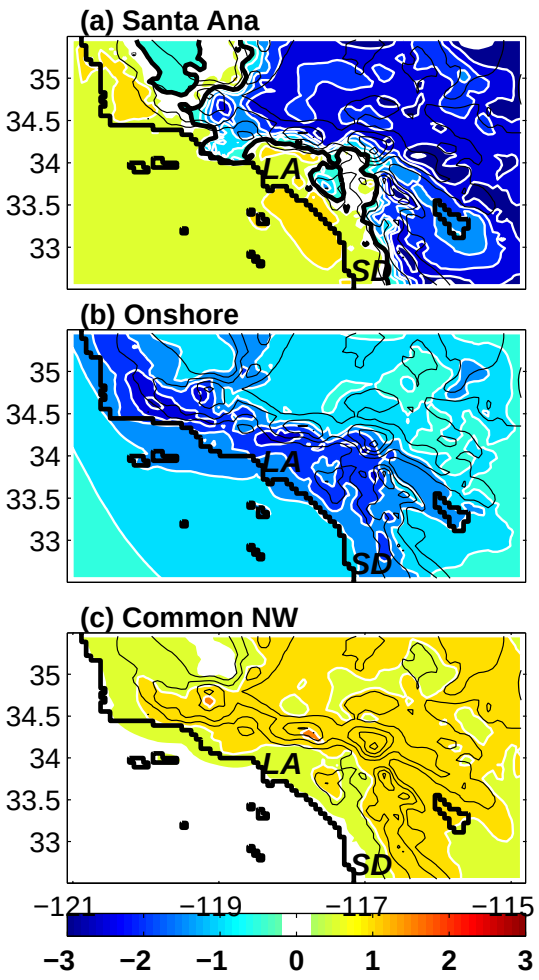

FIGURE 13: Composite 2-m temperature anomaly associated with (a) the Santa Ana regime, (b) the Onshore regime and (c) the Common Northwesterly regime. Units: °C

analysis. We first assess the relationships between local wind regime occurence and indices of the classical large scale teleconnection and weather regimes of the North American and Pacific sectors. We then evaluate the mean atmospheric circulation associated with each of the regimes in terms of SLP and geopotential height.

a. *Coincidence of large-scale modes and local regimes*

In this section we assess the probability that Southern California wind regimes coincide with anomalies of the various large-scale modes of variability prevailing in the North Pacific / North American sector. Here atmospheric variability at intraseasonal and interannual timescales is dominated by a small number of recurrent stationary large-scale flow patterns conceptualized as teleconnections in a linear framework or weather regimes in a non-

linear one. The two phases of the Pacific North American (PNA) pattern have been identified as dominant actors in the two frameworks (Barnston and Livezey, 1987, Kimoto and Ghil, 1993) We examined the coincidence between the local wind regimes and high and low values of the daily PNA index provided by NOAA's Climate Prediction Center. We found that the occurrence of the local wind regimes is uncorrelated with variability of the PNA (see table 1).

We completed the evaluation of the impact of the large scale modes on the local regimes by performing a full EOF analysis of the daily-mean 500 hPa geopotential height anomalies in the North America and Pacific sector (120°E-60°W, 15°-75°N) for the same Oct-Mar seasons. The structures of the four dominant teleconnection patterns identified by the EOF analysis are presented in Fig. 14. These have spatial scales typical of atmospheric Rossby waves, with positive and negative nodes separated by thousands of km, and represent classic teleconnection patterns. For example, EOF3 (Fig. 14c) is very similar to the Pacific/North American pattern of Barnston and Livezey (1987), the correlation of their temporal variations is 0.63.

We then computed the probability of occurrence of each local wind regime when each of the PCs associated with the four large-scale teleconnection patterns of Fig. 14 depart from zero more than 1.2 standard deviations in either the positive or negative direction. For example, to take the case of the Santa Ana regime and the positive phase of EOF1, we computed the number of occurrences of the Santa Ana regime when the PC associated with EOF1 in Fig. 14 is greater than 1.2 standard deviations above the mean. We then divided this by the total number of days when this PC is greater than 1.2 standard deviations above the mean to calculate a probability of occurrence of the Santa Ana regime when the PC of EOF1 is significantly positive. We repeated this for the negative phase of EOF1, and then for the positive and negative phases of the other three EOFs. The result is shown in the left quadrant of Fig. 15. Then we repeated the entire procedure for the Onshore and Common Northwesterly regimes, as well as small number of days left unclassified by the local cluster analysis. These are also shown in Fig. 15.

The overall impression given by Fig. 15 is that none of the large-scale teleconnection patterns, either in their positive or negative phases, is much more likely than any of the others to coincide with a Southern California wind regime. There is some evidence that the negative phase of PC3 and the positive phase of PC4 have an elevated likelihood of being associated with a Santa Ana. This is somewhat consistent with the patterns of Figs. 14c and d, since in the western U.S. these show a low and a high respectively; however, the evidence that even these large-scale modes have much predictive power at the local scale is weak, since the positive phase of PC3 and the negative phase of PC4 also show non-negligible likelihood of being associated with a Santa Ana day. Furthermore in the negative phase of PC3 and the positive phase of PC4, the most likely wind regime is still the Common Northwesterly, followed by the Onshore regime. In fact, the relative probability of occurrence of the Southern California local wind regimes is the same no matter which large scale mode is considered or what its phase is. Of course, the 1995-2003 period is clearly too short to provide reliable statistics on interannual variability. Our conclusion that the large-scale weather modes have little relation with Southern California weather regimes therefore applies only to intraseasonal time scales and shorter.

b. *Large scale circulation associated with local regimes*

While the large-scale atmospheric modes have little relationship with the local Southern California modes, there is a connection between the local modes and larger-scale atmospheric variability, as revealed by the large-scale composite SLP anomalies appearing over the North Pacific and western North America in conjunction with the 3 dominant wind regimes (Fig. 16). The Santa Ana regime is associated with a strong high over the Great Basin. The SLP anomalies accompanying the Onshore regime have a very similar spatial pattern to those accompanying the Santa Ana winds but with reverse sign and weaker amplitude. The Onshore pattern is slightly shifted to the west. A nearly identical pattern emerges from a composite SLP analysis of the days experiencing precipitation, further confirming the tight relationship between the Onshore regime and precipitation. A very similar composite pattern is also related to precipitating days in the Southern Sierra as shown by Pandey et al. (1999). An examination of 500hPa and 200hPa geopotential height fields reveals that the geopotential height counterparts to the SLP anomalies associated with the Santa Ana and Onshore regimes are also found aloft, but are shifted somewhat to the west with increasing height (not shown). Unlike the Santa Ana and Onshore regimes, the Common Northwesterly regime is associated on average with very weak large-scale SLP anomalies (Fig. 16c).

The nearly-opposing SLP patterns of Figs. 16a and b together comprise the most important mode of variability in the southwestern U.S from October to March. For example, the positive and negative phases of the first EOF of the surface pressure anomalies over the largest 54-km domain of our simulation (covering all of the southwestern U.S.) for the same 8 wet seasons

	Negative PNA	Neutral PNA	Positive PNA
Santa Ana	0.10	0.16	0.16
Onshore	0.35	0.28	0.27
Common Northwesterly	0.54	0.54	0.55

TABLE 1: Probability of occurrence of the local wind regimes for negative, neutral and positive PNA large-scale conditions. Negative PNA conditions occur when the PNA index is less than -1 std dev below the mean, while positive conditions occur when the index is greater than 1 std dev above the mean, with neutral conditions falling in between these two cases. The PNA time series was obtained from the NOAA Climate Prediction Center web site (http://www.cpc.ncep.noaa.gov/products/precip/CWlink/pna/pna_index.html)

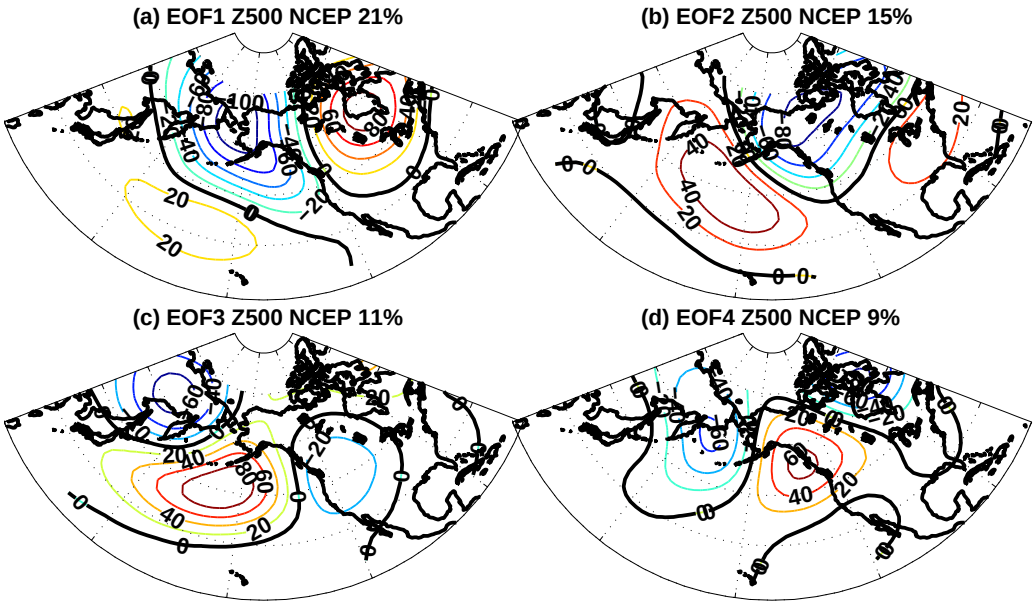

FIGURE 14: EOFs of the daily mean 500-hPa height (Z500) displayed as anomalies regressed on the four leading standardized PC's of daily mean Z500 anomalies over the North America and Pacific sector based on data for the 8 winters 1995-2003. Units: m.

are very similar to the patterns of Fig. 16a and b. It is overwhelmingly the dominant mode of surface pressure variability in the region, accounting for 78% of the variance. The connection between this first mode of the regional-scale pressure variability and the local Southern California winds is also confirmed by the strong correlation (0.73) between it and the first EOF of the Southern California winds shown on Fig. 5.

The regional-scale surface pressure anomalies accompanying the Santa Ana and Onshore regimes (and dominating the regional-scale pressure variability of the southwest U.S.) are qualitatively different from the typical teleconnection patterns thought to govern atmospheric variability. For example, the teleconnection patterns have positive and negative nodes on the spatial scales of Rossby waves (e.g. see Fig. 14). The patterns of Figs. 16a and b, on the other hand, have very little loading of the opposite sign outside the western U.S. and adjacent areas of the Pacific Ocean. Rather than being a wave with positive and negative nodes, these patterns seem instead to represent a standing monopole mode of variability, where pressure vacillates between positive and negative values over a confined area, generating large gradients there with little signature elsewhere.

While the sensitivity of the local Southern California circulation to the pressure of the Great Basin during the Santa Ana and Onshore regimes is striking, equally curious is the insensitivity of the local circulation to larger-scale pressure variability during the Common Northwesterly regime. Though the loading in Fig. 16c is nearly zero everywhere, this is in fact a superposition

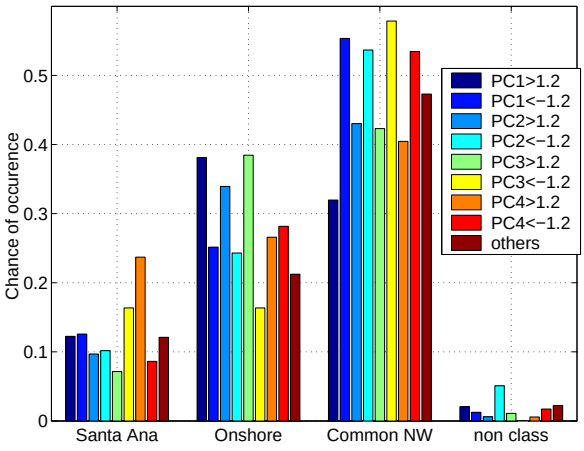

FIGURE 15: Percentage of daily occurrences of the local wind regimes depending on the large scale conditions. The four leading EOF of the Z500 shown in fig. 14 were used to define the large scale conditions, considering only significant departure (1.2 std dev) from the mean of the associated PC.

of a very large variety of large-scale conditions that happen to average to zero, as indicated by the wide variety and phases of large-scale modes coinciding with the Common Northwesterly regime (Fig. 15). Yet the Common Northwesterly regime, as the cluster with the least amount of variability (Fig. 6), is associated with only very small anomalies in the local circulation.

6. Discussion

The primary modes of atmospheric variability in the southern third of California are investigated with a 6-km resolution atmospheric simulation using the MM5 model. An external forcing was imposed on the model's lateral boundaries in the form of the Eta reanalysis from the years 1995-2003, updated every 3 hours. Thus the simulation can be thought of as a reconstruction of Southern California weather and climate over this period, consistent with the physics of the MM5 model and the mesoscale characteristics of the terrain resolved at 6 km. The quality of the reconstructed circulation variability is high, as revealed by the fact that simulated near-surface wind speed and direction both are highly correlated with point measurements of wind speed and direction made at 18 individual stations scattered throughout the model domain. The simulation therefore provides the most accurate and densely-sampled information about Southern California atmospheric circulation available at the present time.

An objective cluster analysis technique applied to simulated daily-mean near-surface winds was used

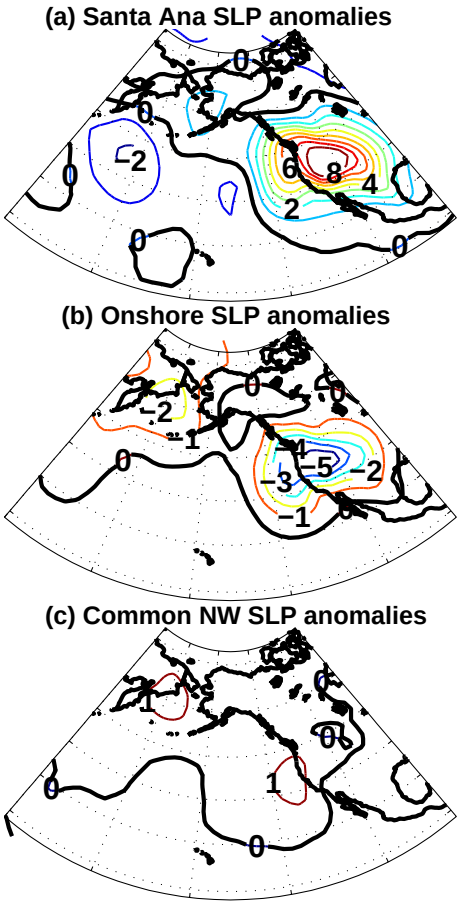

FIGURE 16: Composites of sea level pressure (SLP) anomalies associated with the 3 wind regimes (NCEP reanalysis Oct-Mar 1995 2003). Units: hPa.

to identify the dominant local modes of circulation variability during the October-March wet season. The 'Common Northwesterly' regime, characterized by steady alongshore flow over the ocean and weak winds over land, is the most frequent, accounting for more than half the days. This flow pattern is occasionally perturbed by two other regimes that introduce a strong cross-shore component and are therefore associated with large perturbations in local temperature and hydrology. The 'Onhsore' regime, accounting for slightly less than a third of the days, has a strong onshore component and is also characterized by large variability in the alongshore northwesterlies. The 'Santa Ana' regime, by contrast, is a strong offshore flow, with intense wind speed and gusts in passes and on the slopes of the mountains as air rushes toward the coast from the high desert interior. The Santa Ana days are also characterized by a weakening of the climatological northwesterly alongshore flow. Slightly less than a sixth of the days belong to this regime. The

character of the regimes validates the use of non-linear cluster analysis to identify them. For example, the Offshore and Santa Ana regimes, though opposites in the sense of the cross-shore flow associated with them, are asymmetric in their probability of occurrence, their composite wind patterns, and the variability of the alongshore component of the flow associated with them. This information is impossible to obtain through conventional EOF analysis alone.

These wind regimes, together with the complex Southern California topography, are the main source of highly-structured perturbations in temperature and hydrology in Southern California during the wet season. Under the Onshore regime, flow from the ocean creates cool and moist conditions throughout the region. Lifting of this humid air over the blocked flow which develops on the windward side of the steep slopes of the coastal ranges generates precipitation in the urbanized coastal zone. Orographic enhancement also often yields large precipitation rates on the ocean side of the coastal ranges during the Onshore regime. Precipitation rates are small on the lee side of the coastal range, indicating a rain shadow effect there. The flow originates from the high desert during the Santa Ana regime. While the desert air is originally anomalously cold under this regime, it typically warms enough adiabatically as it descends the coastal slopes to generate a warm anomaly in the low-lying coastal zone. The associated drop in relative humidity is consistently spectacular, so that the urban areas of Southern California experience extreme dryness when this regime occurs. The flow is also strongly accelerated through the passes and along its descent of the coastal ranges, so that the Santa Ana regime is associated with the strongest localized surface wind gusts of any of the three regimes. Under the Common Northwesterly regime, Southern California returns to a stable climate, with little precipitation or winds over land, and modest warmth over most of the land area.

Finally we investigated the relationships between the local wind regimes and the synoptic conditions over the Pacific North America sector. On average, very weak large-scale SLP anomalies accompany the Common Northwesterly regime. The Santa Ana regime is associated with a strong high pressure center over the Great Basin. A synoptic condition with very similar spatial distribution but the opposite sign coincides with the Onshore regime.

While the local climate is particularly sensitive to vacillations of the pressure over the Great Basin region, it is curiously insensitive to the large-scale teleconnections or weather regimes predominant in the Pacific–North American sector. These have minimal impact on the probability of occurrence of the local wind regimes. For example, when the index associated with any particular large-scale teleconnection pattern is high (or low), the probability of occurrence of the three regimes does not change significantly: The Common Nothwesterly is still the most frequent local regime and the Santa Ana and Onshore regimes constitute the dominant perturbations to this state. Thus it makes little sense to speak of the local impacts of the familiar large-scale modes. The local climate is simply not sensitive to the patterns that dominate a coarse-resolution description of large-scale atmospheric variability. Instead it is sensitive to a large-scale pattern that can only be revealed by first identifying local modes and variability and relating them to the larger scale.

In the case of Southern California, the Great Basin pressure anomaly is the critical determinant of the local modes. Thus in trying to predict the sensitivity of this region's modes of variability to a global-scale external forcing such as a future increase in greenhouse gases, attention should be focused on the response of the Great Basin pressure to the external forcing. The unusual sensitivity of local climate to a feature as small as the Great Basin pressure anomaly and its insensitivity to variability elsewhere is also relevant to the interpretation of paleoclimate records of the region (e.g. Roark et al., 2003; Cannariato and Kennett, 2005). These records may not reflect global or even hemispheric-scale climate variability, but may instead reflect the local impacts of variability over the American West.

Our study highlights the potential role of topography in generating and shaping local modes of climate variability and their impacts. Figs. 16a and b reveal that the flows of the Santa Ana and Onshore regimes cross the isobars of the large-scale pressure patterns associated with them. These flows may become ageostrophic because of turbulent dissipation of the large-scale flow by the region's mountain complexes. The Southern California region may be so sensitive to the pressure over the Great Basin because large pressure anomalies in this region align the geostrophic flow most favorably for turbulent dissipation by topography in Southern California. This is of course highly speculative, and is an area for further research. More certain is the role of topography in shaping the local modes once they develop: All of the patterns in Fig. 7 show a great deal of spatial structure clearly related to topography and account for large spatial gradients in windiness and circulation variability in Southern California. And finally, we note the role of topography in determining the spatial structure of the modes' climate impacts. This is particularly apparent in

the modes' highly-localized temperature and hydrology signals in Southern California's urbanized coastal zone. Nestled against the coastal range, this low-lying area is caught in a tug-of-war between ocean and high desert air masses, causing wild swings between the warmth and extreme dryness of the Santa Ana regime and the coolness and rainfall of the Onshore regime. Because of the large role of topography in Southern California climate variability, we conclude that the local perspective we adopt here will be necessary to understand climate variability in other regions of intense topography.

Acknowledgments It is a pleasure to thank M. Hughes for completing the MM5 simulations. The authors are grateful to D. Kondrashov for providing the gaussian mixture model clustering code and to G. Plaut for providing the software used to compute the *k*-means classification. Sebastien Conil would also like to acknowledge M. Ghil for his numerous comments and support.

REFERENCES

Barnston, A.-G. and R.-E. Livezey, 1987: Classification,seasonality and persistence of low frequency atmospheric circulation patterns. *Mon. Wea. Rev.*, **115**, 1083–1026.

Caldwell, P., D. Stuart, and K. Brink, 1986: Mesoscale wind variability near Pt. Conception, California in spring 1983. *J. Clim. Appl. Meteor.*, **25**, 1241–1254.

Cannariato, K. G. and J. P. Kennett, 2005: Structure of the penultimate deglaciation along the California margin and implications for Milankovitch theory. *Geology*, **33**, 157–160.

Cannon, S., 2001: Debris-flow generation from recently burned watersheds. *Env. & Eng. Geosc.*, **7**, 321–341.

Cayan, D. R. and J. O. Roads, 1984: Local relationships between United States West coast precipitation and monthly mean circulation parameters. *Mon. Wea. Rev.*, **112**, 1276–1282.

Dorman, C.-E. and C.-D. Winant, 1995: Buoy observations of the atmosphere along the west coast of the United States, 1981-1990. *J. Geophys. Res.*, **100**, 16029–16044.

Gong, X. and M. B. Richman, 1995: On the application of cluster analysis to growing season precipitation data in North America east of the Rockies. *J. Climate*, **8**, 897–931.

Hall, A. and M. Visbeck, 2001: Synchronous variability in the Southern Hemisphere atmosphere, sea ice, and ocean resulting from the annular mode. *J. Climate*, **15**, 3043–3057.

Hu, H. and W.-T. Liu, 2003: Oceanic thermal and biological responses to Santa Ana winds. *Geophys. Res. Lett.*, **30**, 1596.

Kaihatu, J.-M., R. Handler, G. Marmorino, and L. Shay, 1998: Empirical Orthogonal Function analysis of ocean surface currents using complex and real-vector methodes. *J. Atmos. Ocean. Techn.*, **15**, 927–941.

Keeley, J. and C. Fotheringham, 2003: Impact of past, present, and future fire regimes on North American Mediterranean shrublands. *Fire and Climatic Change in Temperate Ecosystems of the Western Americas*, T. Veblen, W. Baker, G. Montenegro, and T. Swetnam, eds., Springer, New York, 218–262.

Kimoto, M. and M. Ghil, 1993: Multiple flow regimes in the northern hemisphere winter. Part II: sectorial regimes and preferred transitions. *J. Atmos. Sci.*, **50**, 2645–2673.

Kondrashov, D., K. Ide, and M. Ghil, 2004: Weather regimes and preferred transition paths in a three-level quasigeostrophic model. *J. Atmos. Sci.*, **61**, 568–587.

Leung, L.-R. and Y. Qian, 2003: The sensitivity of precipitation and snowpack simulations to model resolution via nesting in regions of complex terrain. *J. Hydrometeorology*, **4**, 1025–1043.

Leung, L.-R., Y. Qian, and X. Bian, 2003: Hydroclimate of the Western United States based on observations and regional climate simulation of 1981-2000.Part I: Seasonal Statistics. *J. Climate*, **16**, 1892–1911.

Ludwig, F., J. Horel, and D. Whiteman, 2004: Using EOF analysis to identify important surface wind patterns in mountain valleys. *J. Applied. Meteorol.*, **43**, 969–983.

Masi, G. and A. Hall, 2005: Coastal blocking and the distribution of precipitation in Southern California. *manuscript in preparation*.

Mass, C., D. Ovens, K. Westrick, and B. Colle, 2002: Does increasing horizontal resolution produce more skillful forecasts? *Bull. Am. Meteorol. Soc.*, **83**, 407–430.

Michelangeli, P.-A., R. Vautard, and B. Legras, 1995: Weather regimes: recurrence and quasi stationarity. *J. Atmos. Sci.*, **52**, 1237–1256.

Neiman, P. J., F. M. Ralph, D. P. Jorgensen, A. B. White, and D. E. Kingsmill, 2004: Modification of fronts and precipitation by coastal blocking during an intense landfalling winter storm in Southern California: Observations during CALJET. *Mon. Wea. Rev.*, **132**, 242–273.

Neiman, P. J., F. M. Ralph, A. B. White, D. E. Kingsmill, and P. O. G. Persson, 2002: The statistical relationship between upslope flow and rainfall in California's coastal mountains: Observations during CALJET. *Mon. Wea. Rev.*, **130**, 1468–1492.

North, G. R., T. L. Bell, R. F. Cahalan, and F. J. Moeng, 1982: Sampling errors in the estimation of Empirical Orthogonal Functions. *Mon. Wea. Rev.*, **110**, 699–706.

Pandey, G. R., D. Cayan, and K. Georgakakos, 1999: Precipitation structure in the Sierra Nevada of California during winter. *J. Geophys. Res.*, **104**, 12019–12030.

Raphael, M.-N., 2003: The Santa Ana winds of California. *Earth Interactions*, **7**, 8.1–8.13.

Redmond, K. T. and R. W. Koch, 1991: Surface climate and streamflow variability in the western United States and their relationship to large-scale circulation indices. *Water Resour. Res.*, **27**, 2381–2399.

Roark, E. B., B. Ingram, J. Southon, and J. Kennett, 2003: Holocene foraminiferal radiocarbon record of paleocirculation in the Santa Barbara Basin. *Geology*, **31**, 379–382.

Smyth, P., K. Ide, and M. Ghil, 1999: Multiple regimes in Northern Hemisphere height fields via mixture model clustering. *J. Atmos. Sci.*, **56**, 3704–3723.

Sommers, W.-T., 1978: LFM forecast variables related to Santa Ana wind occurences. *Mon. Wea. Rev.*, **106**, 1307–1316.

Thompson, D.-W. and J.-M. Wallace, 2000: Annular modes in the extratropical circulation. Part I: Month to month variability. *J. Climate*, **13**, 1000–1016.

— 2001: Regional climate impacts of the Northern Hemisphere annular mode. *Nature*, **293**, 85–89.

Travisña, A., M. Ortiz-Figuerora, H. Herrera, M.-A. Cosio, and E. Gonzalez, 2003: Santa Ana winds and upwelling filaments off Northern Baja California. *Dyn. Atmos. Oceans*, **37**, 113–127.

Westerling, A., D. Cayan, T. Brown, B. Hall, and L. Riddle, 2004: Climate, Santa Ana winds and autumn wildfires in Southern California. *Eos Trans AGU*, **85**, 289–300.

Winant, C.-D. and C.-E. Dorman, 1997: Seasonal patterns of surface wind stress and heat flux over the Southern California Bight. *J. Geophys. Res.*, **102**, 5641–5653.